Abel inversion of soft X-ray fluctuations associated with fast particle-driven fishbone instabilities in MAST plasmas

K.G. McClements[1], J. Young[1,2], L. Garzotti[1], O.M. Jones[1,3], C.A. Michael[4]

[1] *UKAEA, Culham Centre for Fusion Energy, Abingdon, UK*

[2] *University of Bath, Bath, UK*

[3] *University of Durham, Durham, UK*

[4] *University of California Los Angeles, Los Angeles, USA*

Plasmas in the Mega Amp Spherical Tokamak (MAST) were heated principally through the injection of neutral beams which, when ionized, generated fast (supra-thermal) ion populations. These fast ions excited bursting modes with toroidal mode number $n = 1$ whose high frequency (several tens of kHz) combined with a rapid rise and decay in amplitude (on timescales ~2-3ms) led to them being referred to as "fishbones". They were excited when the safety factor q (the number of toroidal circuits made by an equilibrium magnetic field line in one poloidal circuit) dropped to values close to unity in the plasma core. The mode frequency fell ("chirped") during the burst to about the plasma rotation frequency (Fig. 1) and fast ions were expelled from the plasma core region in which the mode was excited. Fishbones were detected in MAST using Mirnov coils and soft X-ray (SXR) cameras. Specifically, line-integrated SXR emission was detected: in the case of the equatorial SXR camera (Fig. 2), this line-integrated emission was the Abel transform of the local emissivity $j(R)$ where R is major radius. Fig. 3 shows equatorial fluctuating SXR emission during the fishbone in Fig. 1 as a function of time and tangency radius of the SXR line-of-sight, p. Here we present calculations of $j(R)$ associated with fishbones in MAST obtained through Abel inversion of measured soft X-ray (SXR) fluctuations.

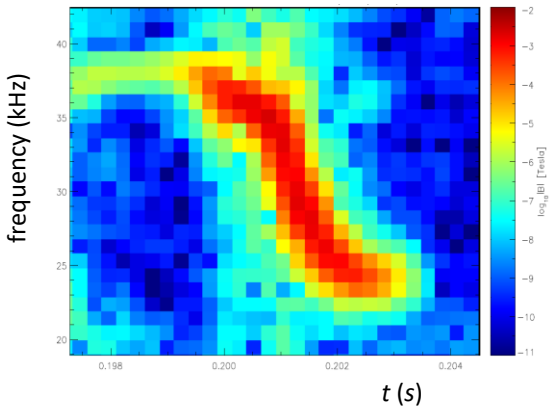

Fig. 1. Spectrogram of Mirnov coil fluctuations for fishbone in MAST pulse 29976.

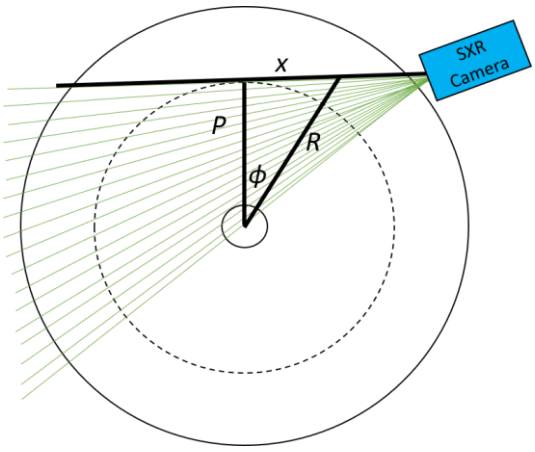

Fig. 2. Equatorial SXR camera lines-of-sight in MAST.

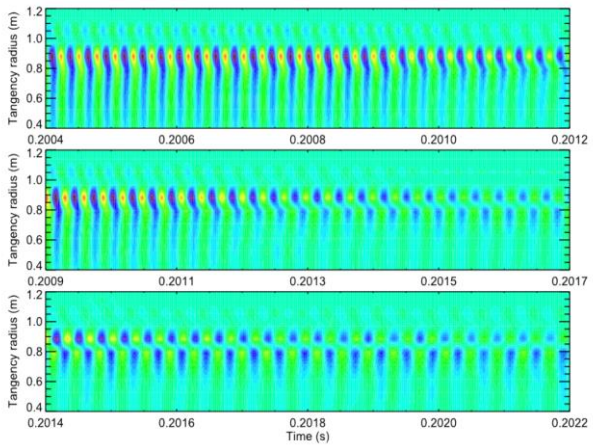

Fig. 3. Fluctuations detected using equatorial SXR camera during fishbone shown in Fig. 1.

SXR emission in MAST is normally assumed to be thermal bremsstrahlung, with emissivity

$$j = J_0 n_e^2 T_e^{1/2} Z_{\text{eff}} e^{-\varepsilon_0/T_e} \qquad (1)$$

where n_e, T_e are electron density and temperature, Z_{eff} is effective ion charge and $\varepsilon_0 \simeq 1\text{keV}$ is the lowest photon energy detected by SXR cameras. Fishbone-induced variations in any of these quantities produce fluctuations in j. Since fishbones have well-defined frequency ω and $n = 1$, their associated SXR emission has space and time dependence

$$j_1(R, \varphi, t) = j_0(R)\cos(\omega t - \varphi) \qquad (2)$$

We define toroidal angle φ such that $\cos(\varphi - \varphi_{pi}) = p_i/R$ where φ_{pi} is constant for the i-th SXR camera line-of-sight (Fig. 1). The fluctuating line-integrated SXR emission is $I_1(p,t) = I_0(p)\cos\omega t$. It can be shown [1] that $I_0(p)\cos\varphi_{pi}/p$ is the Abel transform of $j_0(R)/R$ and hence we can obtain the latter using the inverse transform [2]:

$$j_0(R) = -\frac{R}{\pi}\int_R^\infty \frac{d}{dp}\left(\frac{I_0\cos\varphi_{pi}}{p}\right)\frac{dp}{\sqrt{p^2 - R^2}} \qquad (3)$$

We evaluate this integral using the trapezoidal rule. The SXR data are demodulated through removal of the carrier frequency ω, allowing signals to be aggregated over long periods and hence reducing photon shot noise. A further correction must be applied to take account of systematic phase shifts between different SXR channels. These phase shifts can be obtained by using any SXR channel or Mirnov coil signal as a reference (Fig. 4).

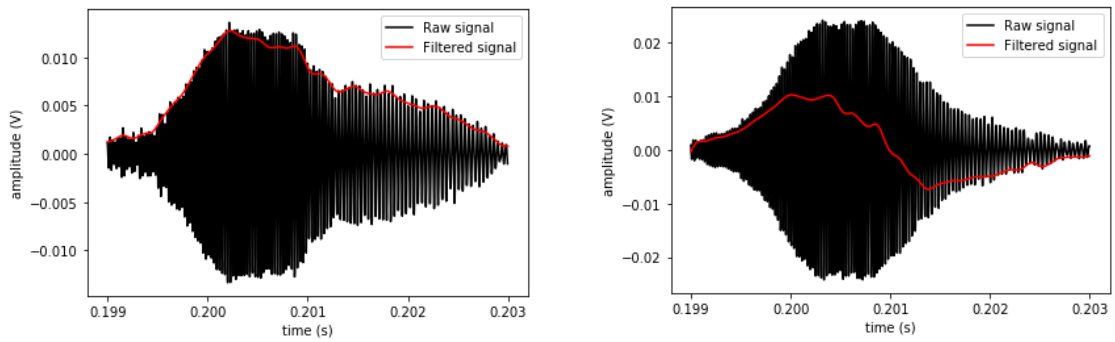

Fig. 4. Raw (black) and filtered (red) signals for MAST equatorial SXR camera channels 11 (left) and 12 (right) during the fishbone shown in Figs. 1 and 3.

The result of applying Abel inversion to the fishbone in Figs. 1 and 3 is shown in Fig. 5. It is possible to define a "phase axis", where the fluctuation amplitude changes sign. During the early phase of the fishbone the phase axis lies outboard of the tokamak magnetic axis $R_0 \approx$ 0.9m. However, in the late phase of the fishbone the phase and magnetic axes coincide (within the spatial resolution of the equatorial soft X-ray camera). The large outboard shift early in the burst does not appear to be compatible with MHD. This behaviour is seen in many other fishbones in MAST and appears to be generic. Fig. 6 shows demodulated SXR emission during the same fishbone obtained using a poloidal array of lines-of-sight. This is close to being up-down anti-symmetric throughout the fishbone, indicating a dominant poloidal mode number $m = 1$.

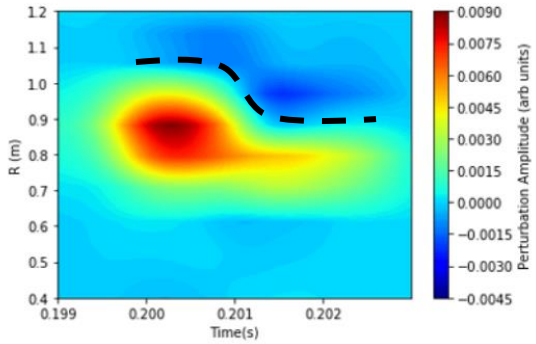

Fig. 5. Contours of $j_0(R)$ for fishbone in Fig. 1 obtained from Abel inversion of SXR data; dashed curve shows phase axis at which j_0 changes sign.

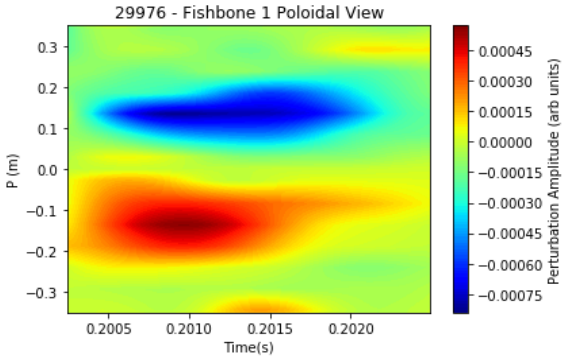

Fig. 6. Demodulated SXR emission due to fishbone in Fig. 1 obtained using poloidal camera ($p < 0$ corresponds to region below midplane).

Fishbones are often characterised as energetic particle modes, meaning that their eigenfunctions are determined primarily by an energetic particle population rather than the thermal plasma. Beams in MAST were normally injected in the co-current direction, so that the beam ions had a large mean toroidal velocity, and it is appropriate to consider a frame co-rotating at rate Ω with these ions. In this rotating frame the effective magnetic field $\boldsymbol{B}$ is modified by the Coriolis force as follows [3]:

$$\boldsymbol{B}_* = \boldsymbol{B} + \frac{2m}{e}\Omega\hat{\boldsymbol{z}} \tag{4}$$

Here $\hat{\boldsymbol{z}}$ is the unit vector in the z-direction and m, e are the beam ion mass and charge. This modification moves the effective flux surfaces to higher R: see Fig. 4 in [4]. The effective magnetic axis is also displaced outboard by an amount given by

$$R_{0,\mathrm{eff}} = \left(1 + 2\frac{\Omega}{\Omega_i}\right) R_0 \tag{5}$$

where Ω_i is the beam ion cyclotron frequency. Putting $\Omega = 10^6$rad s^{-1} (a realistic value) yields $R_{0,\mathrm{eff}} - R_0 \simeq 10$ cm, comparable to the phase axis shift apparent at early times in Fig. 5.

Internal kink modes with $m = n = 1$ are known to be MHD unstable if $q < 1$. Fishbones are believed to be internal kink modes but careful equilibrium modelling seems to indicate that they can occur in plasmas with $q > 1$ [5]: it is not clear how this is possible. Again, the transformation to a frame co-rotating with beam ions may provide an answer: in this frame it is possible to show that the effective safety factor can drop below unity [1], creating the conditions for instability.

We comment finally that the late phase transition of fishbones to MHD-like modes apparent in Fig. 5 could be due to the expulsion of fast ions from the fishbone region. Direct evidence for radial transport of fast ions during fishbones in MAST is provided by drops in both volume-integrated neutron count rates (measured using a fission chamber) and fast ion deuterium-alpha emission from the plasma core [5].

In conclusion, eigenfunctions of fast particle-driven bursting fishbone instabilities in MAST can be obtained through Abel inversion of equatorial soft X-ray emission. A change in the eigenfunction structure can be seen during the course of a fishbone burst: the major radius at which the eigenfunction changes sign is initially outboard of the magnetic axis but moves inboard during the burst. The eigenfunction structure early in the burst can be understood by recognising that the mode is supported by energetic ions with a high average toroidal rotation rate: in a co-rotating frame the magnetic axis is shifted outboard by an amount comparable to the difference between the phase and magnetic axes. We propose that the observed transition to a more MHD-like mode occurs because energetic ions are expelled from the plasma core region where the mode is located. Abel inversion of fishbone soft X-ray emission thus provides insights into the complex interaction of fast ions with thermal plasma.

This work was funded partly by the RCUK Energy Programme [grant number EP/T012250/1]. It was also carried out partly within the framework of the EUROfusion Consortium and has received funding from the Euratom research and training programme 2014-2018 and 2019-2020 under grant agreement number 633053. The views and opinions expressed herein do not necessarily reflect those of the European Commission.

[1] McClements K G *et al* 2021 *Plasma Research Express*, submitted.
[2] Hutchinson I H 1987 *Principles of Plasma Diagnostics* (Cambridge University Press) p124
[3] Thyagaraja A and McClements K G 2009 *Phys. Plasmas* **16** 092506
[4] McClements K G and McKay R J 2009 *Plasma Phys. Control. Fusion* **51** 115009
[5] Jones O M *et al* 2013 *Plasma Phys. Control. Fusion* **55** 085009